ENVIRONMENTAL RESEARCH
LETTERS

LETTER

Inequalities in urban air pollution in sub-Saharan Africa: an empirical modeling of ambient NO and NO_2 concentrations in Accra, Ghana

Jiayuan Wang[1], Abosede S Alli[1], Sierra N Clark[2,3], Majid Ezzati[2,3,4,5], Michael Brauer[6], Allison F Hughes[7], James Nimo[7], Josephine Bedford Moses[7], Solomon Baah[7], Ricky Nathvani[2,3], Vishwanath D[2,3], Samuel Agyei-Mensah[8,11], Jill Baumgartner[9,10], James E Bennett[2,3] and Raphael E Arku[1,*]

[1] Department of Environmental Health Sciences, School of Public Health and Health Sciences, University of Massachusetts, Amherst, MA, United States of America
[2] Department of Epidemiology and Biostatistics, School of Public Health, Imperial College London, London, United Kingdom
[3] MRC Centre for Environment and Health, School of Public Health, Imperial College London, London, United Kingdom
[4] Regional Institute for Population Studies, University of Ghana, Accra, Ghana
[5] Abdul Latif Jameel Institute for Disease and Emergency Analytics, Imperial College London, London, United Kingdom
[6] School of Population and Public Health, The University of British Columbia, Vancouver, Canada
[7] Department of Physics, University of Ghana, Accra, Ghana
[8] Department of Geography and Resource Development, University of Ghana, Accra, Ghana
[9] Institute for Health and Social Policy, McGill University, Montreal, Canada
[10] Department of Epidemiology, Biostatistics, and Occupational Health, McGill University, Montreal, Canada
[11] Department of Civil and Environmental Engineering, Imperial College London, London, United Kingdom
[*] Author to whom any correspondence should be addressed.

E-mail: rarku@umass.edu

Keywords: air pollution, nitrogen dioxide (NO_2), nitrogen oxides (NOx), sub-Saharan Africa, Ghana, air pollution inequality, land use regression

Supplementary material for this article is available online

OPEN ACCESS

RECEIVED
30 August 2023

REVISED
4 February 2024

ACCEPTED FOR PUBLICATION
12 February 2024

PUBLISHED
27 February 2024

Abstract

Road traffic has become the leading source of air pollution in fast-growing sub-Saharan African cities. Yet, there is a dearth of robust city-wide data for understanding space-time variations and inequalities in combustion related emissions and exposures. We combined nitrogen dioxide (NO_2) and nitric oxide (NO) measurement data from 134 locations in the Greater Accra Metropolitan Area (GAMA), with geographical, meteorological, and population factors in spatio-temporal mixed effects models to predict NO_2 and NO concentrations at fine spatial (50 m) and temporal (weekly) resolution over the entire GAMA. Model performance was evaluated with 10-fold cross-validation (CV), and predictions were summarized as annual and seasonal (dusty [Harmattan] and rainy [non-Harmattan]) mean concentrations. The predictions were used to examine population distributions of, and socioeconomic inequalities in, exposure at the census enumeration area (EA) level. The models explained 88% and 79% of the spatiotemporal variability in NO_2 and NO concentrations, respectively. The mean predicted annual, non-Harmattan and Harmattan NO_2 levels were 37 (range: 1–189), 28 (range: 1–170) and 50 (range: 1–195) $\mu g\ m^{-3}$, respectively. Unlike NO_2, NO concentrations were highest in the non-Harmattan season (41 [range: 31–521] $\mu g\ m^{-3}$). Road traffic was the dominant factor for both pollutants, but NO_2 had higher spatial heterogeneity than NO. For both pollutants, the levels were substantially higher in the city core, where the entire population (100%) was exposed to annual NO_2 levels exceeding the World Health Organization (WHO) guideline of 10 $\mu g\ m^{-3}$. Significant disparities in NO_2 concentrations existed across socioeconomic gradients, with residents in the poorest communities exposed to levels about 15 $\mu g\ m^{-3}$ higher compared with the wealthiest ($p < 0.001$). The results

showed the important role of road traffic emissions in air pollution concentrations in the GAMA, which has major implications for the health of the city's poorest residents. These data could support climate and health impact assessments as well as policy evaluations in the city.

1. Introduction

Cities in sub-Saharan Africa (SSA) are in an economic transition and undergoing significant expansion. With such rapid growth, SSA cities are experiencing high levels of air pollution from diverse sources [1]. The growth is also changing the air pollution mixture and the relative roles of the major emission sources. Recent studies suggest that the dominant emission source of urban air pollution in SSA may be shifting from household biomass burning [2, 3] to road traffic [4, 5]. Consequently, while the concentrations of fine particulate matter pollution ($PM_{2.5}$) are showing signs of plateauing [4], several studies are reporting steady increases in oxides of nitrogen (NO_x) pollution [5–8], which are markers of traffic emissions in cities. Increasing formal and informal industrial activities as well as household and commercial use of diesel generators are also common in SSA cities and contribute substantially to ambient NO_x levels. The distribution of these sources in relation to land use and socioeconomic factors influences the spatial patterns of NO_x pollution in local communities [4, 5, 9–14]. For cities across the West African sub-region, seasonal changes in regional meteorological parameters (e.g. mixing layer depth, incident solar radiation and water vapor mixing ratio) during the dry and dusty Harmattan may also amplify NO_x concentrations from local emissions during this period [5, 11, 12]. Yet, there is a dearth of long-term monitoring data for understanding trends, space-time variations and inequalities in combustion related emissions and exposures at city-scale in SSA, one of the world's fastest urbanizing regions.

Nitrogen dioxide (NO_2), the largest component of NO_x, is associated with adverse health impacts such as inflammation of the airways and impaired lung function [15, 16]. Along with NO_x, NO_2 reacts with other chemicals in the air to form PM and ozone (O_3). These photochemical reactions can also produce adverse impacts on the environment (e.g. formation of haze, smog, and acid rain). As such, national governments and international agencies have set health-based guidelines to reduce NO_x emissions. Furthermore, NO_2 is regularly monitored in cities in high-income countries. This is not the case in most sprawling cities in SSA, though the vehicle fleets contain high volumes of older, more polluting vehicles. Furthermore, because urban growth in SSA is largely unplanned, places with quality and healthy living environments are unequally distributed within cities. Although there are global satellite data on NO_2 pollution covering the region [17], they do not capture the high within-city variability that characterizes localized emissions and sources in the context of SSA. To create accountability towards equitable urban living environments, local fine-scale data are needed for regulatory purposes as well as to identify and support deprived populations and communities. Such data are equally essential for health and climate impact assessments at the local community level in an exposure setting that is quite different from those in high-income country cities [18, 19]. In particular, NO_x data, when combined with increasing data on $PM_{2.5}$ and black carbon (BC), will deepen our understanding of the shifting emission sources that is happening in SSA cities that are in economic transition. The data will also enable SSA cities to design and implement integrated air quality management schemes to address growing urban air pollution problems in the region. Additionally, NO_2 emissions serve as a general proxy for co-emitted pollutants (e.g. carbon monoxides and heavy metals) during fossil fuel combustion. Hence, knowledge of the patterns and concentrations of NO_2 gives added information from the environmental justice perspective.

Previously, we described the levels and patterns of nitric oxide (NO) and NO_2 pollution using year-long measurement data on NO_x ($n = 428$ weekly samples) and NO_2 ($n = 472$ weekly samples) from 134 monitoring sites in Accra, Ghana [5]. In this paper, we leveraged the measurement data to develop empirical (so called 'land use regression') models to map ambient NO and NO_2 concentrations at fine spatiotemporal scales (weekly at 50 m) over the entire city. Model predictions were used to derive population exposure distributions and as well to investigate socioeconomic disparities in exposure across the metropolis. We are aware of only two small studies that mapped NO_2/NO in SSA, but none in a large metropolis like Accra [20, 21].

2. Methods

2.1. Study area

Accra is one of the largest and fastest-growing metropolises in West Africa. Our study was conducted in the Greater Accra Metropolitan Area (GAMA), the capital of Ghana and home to an estimated six million residents [22]. GAMAs 1500 km^2 area contains multiple administrative districts, including the city core and most populous Accra Metropolitan Area (AMA);

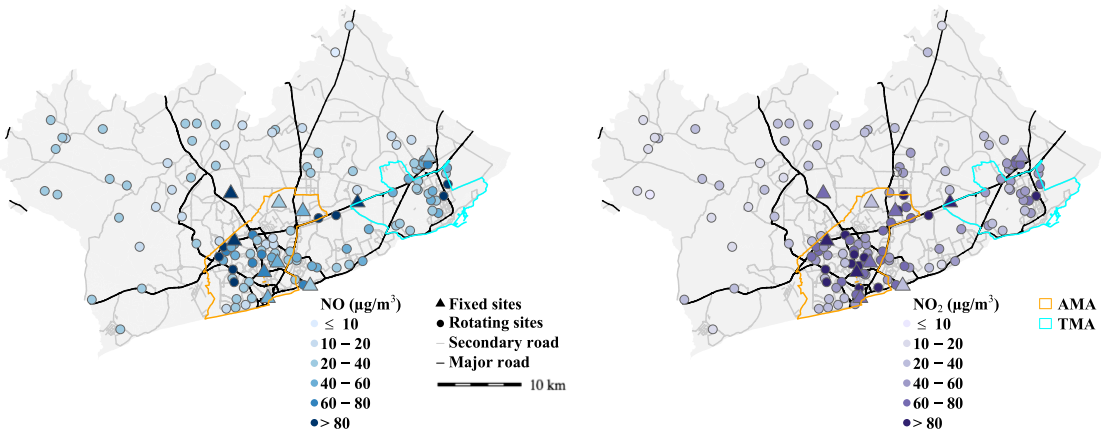

Figure 1. Map of the Greater Accra Metropolitan Area (GAMA) with locations of '*fixed*' and '*rotating*' sites with annual concentrations of (A) NO and (B) NO_2. The colors of NO_2 concentrations indicate comparison to the new World Health Organization (WHO) annual air quality guideline of 10 μg m^{-3}. The concentrations at the fixed sites represent annual mean values, and the rotating sites represent season-adjusted mean values (i.e. an estimated annual means). Major and secondary road network were from OpenStreetMap [27] (downloaded in 2019).

and the Tema Municipal Area (TMA), the industrial hub and seaport situated east of AMA. Daily commute in the GAMA is characterized by heavy traffic congestions, with cars and 'trotro' (minibuses for public transport) alongside pedestrians [23]. There is limited formal bus transit and train services. Recently, there is a growing number of subcompact cars being used as ride-shares such as Uber and Bolt, and the use of motorcycle-taxis ('Okada') is on the rise. To fill the insufficient energy access gap in this growing economy, household and commercial use of diesel generators is commonplace. These are all sources of NO_x emissions in the city. Despite the economic and technological advancement, there still exists immense inequalities in income, housing, infrastructure, and services, which also pattern disparities in environmental pollution within the city. The GAMA experiences two major seasons: the dry and dusty Harmattan (November to February), where north-easterly trade winds blows in mineral dusts from the Sahara Desert during a stagnant local meteorology; and the wet/rainy season (May to October), generally dominated by local air pollution sources [4, 5, 11, 12].

2.2. Data sources

2.2.1. NO_2 and NO_x measurement

Detailed description of the measurement campaign and site selection can be found elsewhere [5]. Between April 2019 to June 2020, we collected weekly integrated NO_2 and NO_x samples at 134 unique sampling locations using Ogawa passive samplers. The 134 sites were chosen to cover diverse land use and socioeconomic status (SES) in the GAMA. As frequently used markers for traffic-related emission, we expected a high degree of inter- and intra-neighborhood variations in NO_x pollution within GAMA. Thus, our sampling sites were over-represented in the more densely populated AMA relative to the rest of the GAMA, as a reflection of the population, land use and source features. Ten of the sites were sampled weekly for one year to capture longer-trend ('*fixed sites*') and 124 sites were sampled for one week each to allow for wider geographic coverage ('*rotating sites*') (figure 1). There were some missing data between March and April 2020, due to Covid-19 lockdown of Accra as well as mandatory quarantine for the field team through contact tracing. While Covid-19 partial lockdown affected emissions in the city briefly, but our analysis showed that the levels rapidly returned to pre-lockdown concentrations in the post-lockdown era[5]. Altogether, we collected a total of 428 and 472 weekly NO_x and NO_2 samples, respectively, comprising 281 NO_2 and 251 NO_x samples in the pre-Covid-19 lockdown, 19 pairs during Covid-19 lockdown, and 50 pairs in the post-Covid-19 lockdown periods. We collected field blank and duplicate samples at 20% of the rotating sites. All the raw data were blank-corrected, and the duplicates had good agreement ($R^2 = 0.98$ for NO_x; and 0.95 for NO_2) [5]. We did not collocate the Ogawa samplers against a reference NO_x/NO_2 monitor as they had been well-characterized in field settings with good agreements [24, 25], including in similar settings as ours [26]. We estimated NO from NO_x as $NO = NO_x - NO_2$. The final weekly estimates were converted using temperature and relative humidity (RH) of that measurement week. We reported all results in μg m^{-3} (1ppb $NO_2 \approx 1.88$ μg m^{-3} and 1 ppb NO ≈ 1.23 μg m^{-3}, all the conversion factors between ppb and μg m^{-3} were calculated based on weekly measured temperature and RH) for easy comparison with other studies and international health guidelines.

Full description of the NO and NO_2 analysis and concentrations at the monitoring sites is available elsewhere [5]. In summary, NO and NO_2

concentrations varied spatially (i.e. by land-use features) and temporally (by season), with annual mean for NO_2 well above international health-based guidance (figure 1). The measured data were strongly associated with indicators of road traffic emissions and meteorological variables.

2.2.2. Predictor variables

We gathered spatial and temporal predictor variables that reflect emissions and factors related to sources in the SSA urban environment (table 1). We first created four buffer sizes (50 m, 100 m, 200 m and 500 m) around each of the 134 sites. Within each buffer, we extracted multiple spatial predictor variables related to traffic (road network) emissions, land use, population, and human activities as described below in model selection. We used a road network shapefile from OpenStreetMap [27] (downloaded 2019) to estimate total length of major and secondary roads; distance from the monitor to the nearest major and secondary roads; and counts of bus/trotro stations/terminals. Total length of waterways (river, stream, canal and drain) were also estimated. We used Spot five imagery (2014) to calculate total area of land within each buffer that were characterized as commercial/business/industrial; high-density residential; low-density residential; and peri-urban background. Normalized difference vegetation index (NDVI) from Landsat-8 satellite imagery was used to characterize vegetation within each buffer size. Additionally, we used the 2010 national census data to compute population density and the share of households using biomass in each census EA, the smallest spatial administrative unit. Further, human activity data, including restaurants, bars, shops, schools, hospitals, churches, and mosques were retrieved from Google places in 2020. We could not find any reliable data on trash burning, fish smoking, generator use, traffic volume, and industrial emissions.

SSA's unique periodic changes in meteorology play an important role in worsening air quality, especially during the Harmattan season. Thus, we also considered several temporal predictor variables to investigate the role of meteorology on NO and NO_2. We measured weather parameters at several sites using Kestrel 5500 (Nelsen-Kellerman, Pennsylvania, USA) and computed the averaged mean temperature, RH, and wind speed for each measurement week. But the weekly averaged values showed minimal spatial variations across sites, thus, we relied solely on weather data from a fixed background site as a representative site. Using the Global Data Assimilation System from the National Oceanic and Atmospheric Administration (NOAA) [32], we computed averaged median mixing layer depth, median incident solar radiation, and mean water vapor mixing ratio at the fixed background site for each measurement week. Daily rainfall data at the Kotoka international airport were used to calculate the number of days it rained in each measurement week.

2.3. Model development

Most previous land use regression models relied solely on spatial predictors and could not capture the temporality that is inherent in environmental exposures [33–38]. In this study, we applied mixed effects linear regression models to examine the associations of weekly NO and NO_2 concentrations with both the spatial and temporal factors [39]. To capture time-dependent variance, we added calendar-month and calendar-week as fixed and random effects, respectively. An indicator for measurement sites was also included as random effects to account for both repeated measurements at the fixed sites and site-specific unmeasured factors.

Like previous studies [40, 41], the weekly ambient NO and NO_2 concentrations at measurement site i on week j is assumed to be a linear function specified as:

$$\mathrm{NO}x_{ij} = \alpha_0 + \beta_1 X_i + \beta_2 \mathrm{Met}_j + \beta_3 \mathrm{Mon} + b_i + \gamma_j + \varepsilon_{ij}$$

where $\mathrm{NO}x_{ij}$ is the concentration of NO or NO_2 measured at location i in week j; α_0 is the fixed intercepts, β_1, β_2, and β_3 are the regression coefficients; X_i is a vector of individual spatial predictor variables assembled in table 1 at site i; Met_j is the meteorology data in week j; Mon is the calendar month for week j; b_i and γ_j are the random intercepts of site and week; and ε_{ij} is the error term.

2.3.1. Model selection

Our model selection process was aimed at finding parsimonious and generalizable set of predictors with maximum predictive accuracy. We first conducted univariate analysis for all the predictor variables (figures S1 and S2). For each spatial variable, we selected the buffer size with the highest correlation (Pearson r) with NO and NO_2 (figures S3 and S4). We then used a supervised stepwise forward regression selection approach to determine the optimal models. The predictors with the highest adjusted R^2 were added sequentially to the model and retained if our *a priori* direction of association was confirmed and there was at least 1% gain in the adjusted R^2 (table S1) [35, 42]. Finally, we checked collinearity; variables with variance inflation factor (VIF) > 3 were removed and the model was rerun. All analyses and model development were implemented with the open-source statistical package R version 4.1.2 (R Project for Statistical Computing). R package 'lme4' was used to fit the mixed effects models.

2.3.2. Model validation

A commonly used technique in statistics (or machine learning) to assess the performance and generalizability of a newly developed predictive models is to examine how well the model will perform when predicting at unseen location [43, 44] (i.e. locations in

Table 1. Candidate predictor variables available for model selection.

Variables and categories	Unit	Buffer size (m)	Source
Traffic variables			OpenStreetMap (2019) [27]
Total length of major roads	m	50, 100, 200, 500	
Total length of secondary roads	m	50, 100, 200, 500	
Distance to the nearest major road	m	—	
Distance to the nearest secondary road	m	—	
Land use variables			World Bank [28] 20 m × 20 m
Commercial/business/industrial	m^2	50, 100, 200, 500	
High-density residential	m^2	50, 100, 200, 500	
Low/medium-density residential	m^2	50, 100, 200, 500	
Peri-urban areas	m^2	50, 100, 200, 500	
Normalized difference vegetation index (NDVI)	—	50, 100, 200, 500	United States Geological Survey [29]—Landsat 8 imagery (30 m × 30 m)
Waterways (total length)	m	50, 100, 200, 500	OpenStreetMap [27, 2019]
Counts of building	N	50, 100, 200, 500	Maxar/Ecopia.ai [30, 2020]
Population			Ghana census (2010) data [31]
Biomass use	%	50, 100, 200, 500	
Population density	pop km^{-2}	50, 100, 200, 500	
Human activities			Google Places (retrieved in 2020)
Number of restaurants	N	50, 100, 200, 500	
Number of schools	N	50, 100, 200, 500	
Presence of bars	N	50, 100, 200, 500	
Presence of shops	N	50, 100, 200, 500	
Meteorological variables			
Temperature	˚C	—	Kestrel weather meters
Relative humidity	%	—	Kestrel weather meters
Wind speed	m s^{-1}	—	Kestrel weather meters
Mixing layer depth	m	—	HYSPLITE model [32]
Solar radiation	W km^{-2}	—	HYSPLITE model [32]
Water vapor mixing ratio	kg kg^{-1}	—	HYSPLITE model [32]

N: number.

the GAMA other than the 134 measurement sites). Thus, the fit and external predictive power of our final models were evaluated using 10-fold CV [40–42, 45–47]. First, all the samples were randomly allocated into 10 subsets, each containing 10% of the data. Subsequently, by holding out a 10%, the remaining 90% was used to train the model and predict the 10% hold-out data. The process was repeated so that every group was used one time in the validation process. For each iteration, we evaluated model performances by computing the mean absolute error (MAE), root-mean-square error (RMSE) as well as *R*-square (R^2) between the predicted and the measured values. Our final NO and NO_2 models are summarized in table 2, and their performances in table 3.

Model R^2s fixed effects (spatial-invariant) and random effects (time-varying) variables in the mixed effects regression. We estimated RMSE as RMSE $= \sqrt{\frac{\sum_{i=1}^{n}(y_i - x_i)^2}{n}}$, where y_i is the predicted value, x_i is the observed value; n is the total number of data points; and MAE as MAE $= \frac{\sum_{i=1}^{n}|y_i - x_i|}{n}$, where y_i is the predicted value, x_i is the observed value; n is the total number of data points. CV. We reported information separately for the fixed only ('Fixed') and the combined fixed and random 'Mixed' components of the models.

2.3.3. Model prediction, population exposure and socioeconomic inequalities in exposure

The final models were used to predict weekly NO and NO_2 concentrations at 50 m × 50 m resolution across the entire GAMA, using *st_as_stars()* function in the '*stars*' package in *R*. We then generated the same variables in the final model within each grid. The model was run for each grid for each calendar week. The weekly predictions were then summarized and mapped as annual and season-specific (non-Harmattan vs Harmattan) mean concentrations. We also used the predictions to estimate the share of population in the AMA that were exposed to NO_2 concentration relative to the World Health Organization (WHO) guidelines. This was done by spatially overlaying the predicted NO_2 concentration surfaces onto 2010 census EA map and summarizing the predicted NO_2 by the share of population in each EA. We relied on the 2010 census because Ghana's 2021 census

Table 2. Associations of measured NO_2 and NO concentrations with spatial and temporal predictor variables in the final linear mixed models.

NO_2			NO		
Predictor variables	Buffer size (m)	Coefficient (Std. error)	Predictor variables	Buffer size (m)	Coefficient (Std. error)
Intercept	—	40.1 (5.9)	Intercept	—	61.8 (5.4)
Length of major road[a]	100	5.6 (2.8)	Length of major road[a]	100	23.4 (3.5)
Length of secondary road[a]	200	10.4 (2.4)	Length of secondary road[a]	50	15.8 (2.7)
NDVI[a]	50	–13.7 (1.6)	Presence of bar[a]	500	3.3 (1.8)
Mean wind speed in calendar week[a]	—	–11.0 (1.7)	Mean solar radiation in calendar week[a]	—	−4.0 (2.1)
Mean RH in a calendar week[a]	—	–4.1 (1.4)			
Calendar month			Calendar month		
July 2019	—	28.9 (7.3)	July 2019	0	0
August 2019	—	27.7 (7.7)	August 2019	—	–4.4 (6.0)
September 2019	—	22.2 (7.3)	September 2019	—	9.3 (7.4)
October 2019	—	13.4 (6.9)	October 2019	—	–1.5 (6.4)
November 2019	—	17.7 (6.8)	November 2019	—	–9.1 (7.2)
December 2019	—	24.4 (8.5)	December 2019	—	–12.9 (8.9)
January 2020	—	20.1 (11.3)	January 2020	—	–26.7 (13.2)
February 2020	—	26.9 (7.0)	February 2020	—	–4.0 (7.7)
March 2020	—	14.5 (7.1)	March 2020	—	–12.9 (7.0)
April 2020	0	0	April 2020	—	–35.3 (11.1)
May 2020	—	12.0 (7.6)	May 2020	—	–3.5 (7.1)
June 2020	—	17.9 (8.9)	June 2020	—	0.3 (8.8)

[a] Standardized: Continuous variables were standardized by subtracting the mean and dividing by the standard deviation. A 1-point change in a standardized variable corresponds to a 1 standard deviation increase on the original scale.

Table 3. Model fit and 10-fold cross validation between the predicted and the measured samples.

	Model R^2				
Model	Fixed	Mixed	RMSE ($\mu g\ m^{-3}$)	MAE ($\mu g\ m^{-3}$)	R^2_{CV} (%)
NO	0.66	0.79	21.7	14.9	0.78
NO_2	0.62	0.88	14.6	10.8	0.80

results were not available at the time of this analysis. Here, we focused on AMA as it is the most urbanized and densely populated and the commercialized hub of the GAMA. We chose NO_2 for this additional analysis because it is a key marker for traffic-related air pollution in cities, and concerns over its adverse health and environmental impacts have resulted in national regulations and international guidelines to minimize population exposures. Unlike NO_2, NO does not have regulatory guidance.

Similarly, we investigated whether NO_2 distribution varies by EA level SES in the AMA. Our measure of SES was median household consumption estimated from the 2012 Ghana Living Standard survey combined with the 2010 census, using small area models. Detailed description of how the area-level SES was calculated can be found elsewhere [48]. The EAs were divided into SES quintiles (i.e. 20% of EAs in each group) to represent low-, medium-low-, medium-, median-high-, and high-SES groups. The median NO_2 levels across the different SES groups were then compared. We also conducted t-test to assess the mean difference in the averaged NO_2 concentrations between the highest vs lowest SES groups, using a p-value cut-off of <0.05.

3. Results

3.1. Final models and their performance

Table 2 summarizes the final NO and NO_2 models. The NO model included length of major (within 100 m) and secondary (within 50 m) roads, presence of bars (within 500 m), and mean solar radiation in a calendar week, which explained 79% of the variability in measured NO ($R^2 = 0.79$). The NO_2 model included length of major (within 100 m) and secondary (within 200 m) roads, NDVI (within 50 m), mean wind speed and RH in a calendar week, explaining 88% of variability in NO_2 ($R^2 = 0.88$) concentrations. CV results showed strong correlation between the predicted and the measured NO ($R^2_{CV} = 0.78$) and NO_2 ($R^2_{CV} = 0.80$) concentrations, respectively (figure 2). Both RMSE and MAE for NO (21.7 and 14.9 $\mu g\ m^{-3}$, respectively) and NO_2

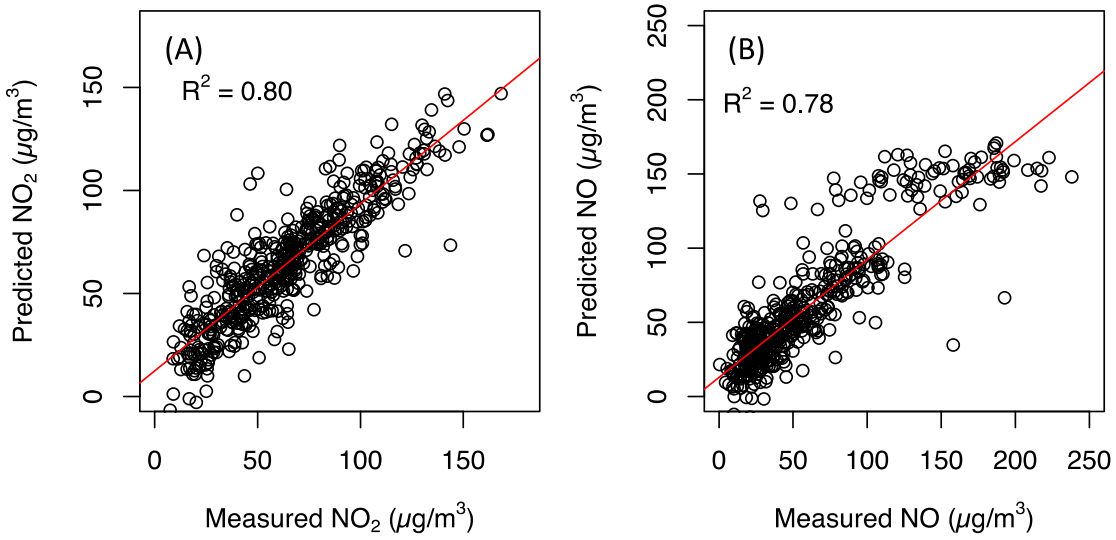

Figure 2. Scatter plots of the measured vs. predicted (A) NO_2 and (B) NO concentrations based on 10-fold cross-validation.

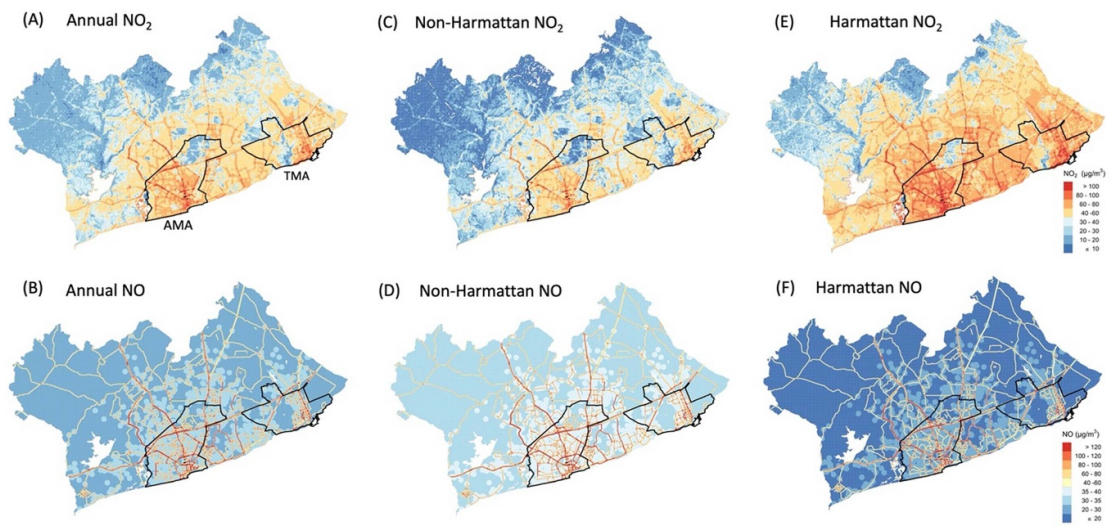

Figure 3. Estimated (A) and (B) annual, non-Harmattan (C) and (D), and Harmattan (E) and (F) NO_2 and NO concentrations in the GAMA.

(14.6 and 10.8 $\mu g\ m^{-3}$, respectively) were relatively small if compared with the range of measured concentrations. The VIF values for both models were <2, suggesting little collinearity among variables in the final models. Nevertheless, the NO model performed better at concentrations <150 $\mu g\ m^{-3}$ than at higher (>150 $\mu g\ m^{-3}$) concentrations (figure 2(B)). This could be due to the fewer number of observations with extremely high concentrations in our dataset (figure 2(B)).

3.2. Spatial and temporal patterns of NO_2 and NO concentrations

Predicted annual, non-Harmattan, and Harmattan mean NO_2 and NO concentrations are represented in figure 3, with summary statistics in table 4. The predicted mean (standard deviation, SD) annual NO_2 concentration for the entire GAMA was 37 (19) $\mu g\ m^{-3}$ and ranged from less than 10 $\mu g\ m^{-3}$ in the vegetated peri-urban areas to over 180 $\mu g\ m^{-3}$ in high traffic areas. The highest NO_2 levels were concentrated within the city core and along and around major roads in the AMA and TMA (figures 3(A)–(E) and 4(A)–(C)). The mean annual NO_2 concentration (60 $\mu g\ m^{-3}$) in the more congested AMA was nearly doubled that of the entire GAMA. Similarly, the port city district of TMA showed relatively higher NO_2 concentration compared to the entire GAMA (figure 4(C)). Both AMA and TMA have the highest vehicular traffic congestions in Ghana.

Predicted NO concentration across the GAMA showed less spatial heterogeneity but steeper gradient compared with NO_2. The highest concentrations appeared along road networks, with clusters of relatively high levels in locations with bars

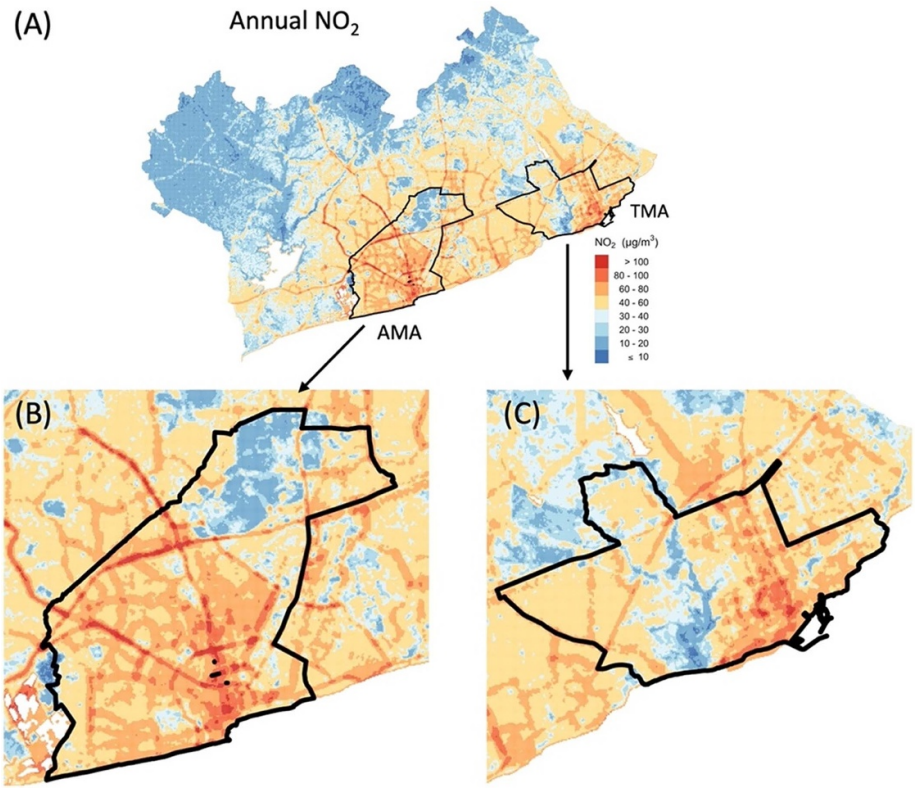

Figure 4. Estimated (A) annual NO_2 in the GAMA with zoom in for (B) AMA and (C) TMA.

Table 4. Predicted NO_2 and NO concentrations (μg m^{-3}) in the GAMA, AMA and TMA.

		Annual		Harmattan		non-Harmattan	
Area	Pollutant	Mean (SD)	Range	Mean (SD)	Range	Mean (SD)	Range
GAMA	NO_2	37 (19)	1–189	50 (22)	1–195	28 (18)	1–170
	NO	34 (23)	24–514	23 (23)	13–503	41 (23)	31–521
AMA	NO_2	60 (20)	1.2–179	75 (21)	1.24–195	51 (20)	1–170
	NO	55 (42)	24–514	44 (42)	13–503	62 (42)	31–521
TMA	NO_2	53 (18)	1–131	68 (20)	1–147	44 (18)	1–122
	NO	43 (30)	24–319	32 (30)	13–308	49 (30)	31–325

(figure 3(B)). These results point to traffic as the most important source of NO emissions in Accra, with additional contributions from commercial biomass and/or generator use. NO is known to oxidize to NO_2 very quickly, which could explain the steep gradient in NO concentrations away from the major roads. At the same time, this reaction could be responsible for the higher NO_2 levels in the more urbanized and industrialized areas of the GAMA. Like NO_2, the annual NO concentrations across the city varied more than one order of magnitude, with overall mean of 34 μg m^{-3} (table 4).

By season, mean NO_2 concentrations were higher in the Harmattan period than the non-Harmattan, increasing overall by about 80% across GAMA and between 50%–60% in AMA and TMA (table 4). The opposite was true for NO, where the levels during the Harmattan were about 50% lower than in the non-Harmattan.

3.3. Population exposure to NO_2 concentration in the AMA

The predicted NO_2 levels for all residents of AMA exceeded the WHO health-based guideline of 10 μg m^{-3}, regardless of the season (figure 5). Most of the population in the AMA (80%) lived in areas with annual NO_2 concentration 5–8 times the recommended guideline (table S2). In the dusty Harmattan season when pollution was highest, over half (56%) of the population lived in areas where NO_2 concentrations were above 80 μg m^{-3}. Though pollution levels improved during the wet non-Harmattan period, still almost 80% of the residents experienced NO_2 concentrations 4–7 times the recommended guideline.

In terms of SES, while exposure in both rich and poor communities were above the WHO guideline, there still was a clear gradient in the median NO_2 concentrations across the EA SES quintiles in the

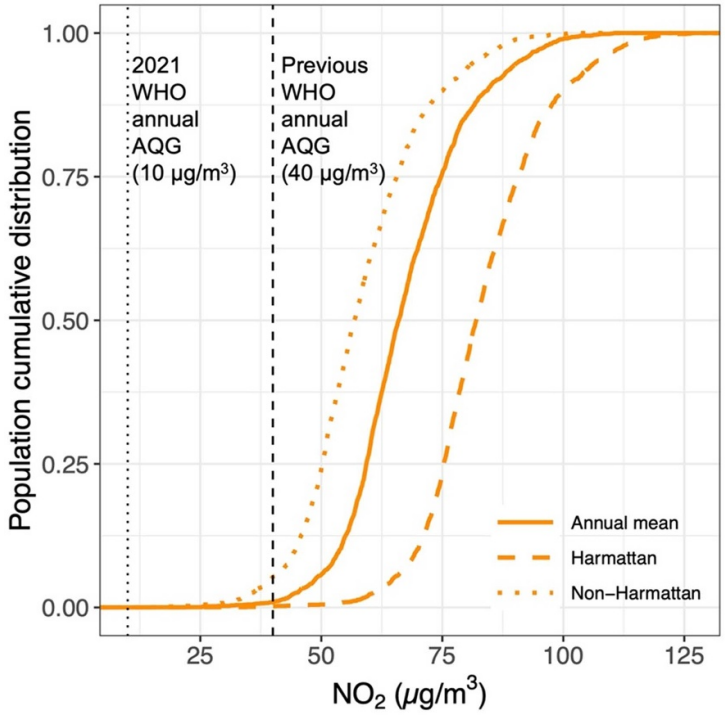

Figure 5. Cumulative densities of the proportion of AMA population living in enumeration areas (EAs) with varying NO_2 concentration relative to the WHO guideline, by annual, Harmattan, and non-Harmattan averages. The population data used was from the 2010 Ghana Census. The vertical black dash/dotted-lines show the previous (40 μg m^{-3}) and the recently revised (10 μg m^{-3}) World Health Organization (WHO) annual air quality guideline (AQG) for NO_2.

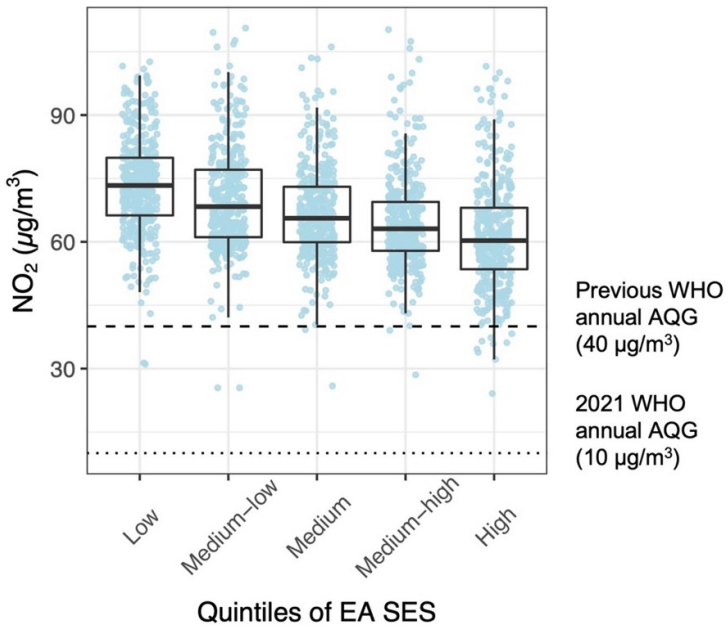

Figure 6. Distribution of enumeration area (EA) annual mean NO_2 concentrations within quintiles (20% increments) of EA socioeconomic status (SES) in the Accra Metropolitan Area (AMA). SES: EA median log equivalized household consumption. The upper and lower limits of the black box represent the interquartile range of the distribution and the horizontal line within the box represents the median. Each colored point represents an EA average NO_2 level (μg m^{-3}).

AMA (figure 6 and table S3). The poorest neighborhoods had statistically significantly higher exposure compared the wealthiest (73 vs 60 μg m^{-3}; $p < 0.001$).

4. Discussion

As SSA rapidly urbanizes, air quality in cities will have major health implications for urban residents. We

leverage large-scale measurement data to map out NO and NO_2 concentrations at 50 m spatial and weekly time resolution over the entire GAMA, one of SSA's fastest urbanizing metropolises. The final models had high predictive performance and explained much of the variability in the measured NO and NO_2 concentrations. Road traffic variables were the most important spatial predictors in both models, especially for NO, signifying the role of fresh traffic emissions in the GAMA. This resulted in relatively higher concentrations in the more congested AMA and TMA. We also found a strong negative correlation between greenness NDVI and NO_2 concentrations in the city, indicating the potential mitigative effect of vegetation in reducing NO_2 pollution [49]. NDVI in Accra could be closely linked with SES as wealthier communities tend to have more trees than poorer ones. Also, trees/green spaces are known to regulate microclimate by moderating air temperature and humidity, both of which have significant influence on NO_2 formation and retention. Our finding of the negating role of NDVI points to the need for planting more trees in this sprawling city. Increasing urban green spaces in general can contribute to localized improvements in overall air quality, particularly in areas with high traffic or industrial emissions. For a typical SSA city, residential biomass fuel use could be an important emission source for NO and NO_2. However, using the 2010 national census data, neither of our final models included household biomass use as an important predictor variable. Interestingly, location of bars (including restaurants) was predictive of NO levels in Accra. This could indicate either commercial biomass use for cooking for sale, the use of disease generators power generation or the presence of cars from customers. Time-varying meteorological variables, including solar radiation (for NO) and wind speed and RH (for NO_2) were also important predictors. Seasonal changes in these variables produced opposite effects on NO_2 and NO concentrations in the GAMA. NO_2 concentrations were higher in the hot, dry and dusty Harmattan period than in the wet/rainy non-Harmattan season. This could potentially be due to more active photochemical and/or aqueous oxidation favored by the meteorological conditions such as stronger solar radiation, and relatively high RH [5], thereby enhancing secondary formation of NO_2 from NO. Nonetheless, the entire residents of the AMA were exposed to NO_2 levels exceeding the WHO guideline of 10 μg m^{-3}, regardless of the season, with the poorest neighborhoods at much higher risk of exposure than the wealthiest. As Accra expands, there is a need to understand and intervene on factors which drive socioeconomic inequalities in emissions and exposures.

Two studies that empirically mapped NO_2 levels in SSA were conducted in small urban areas in Ethiopia [20] and Mauritania [21], where the annual mean concentrations were between 5–10 times lower than seen in Accra. To our knowledge, this is the first temporally resolved NO and NO_2 models developed for a major SSA city, thus we could only compare our models broadly with studies from high-income regions while noting that both the physical and policy environments between the two are completely different. Further, there are limited space-time NO_x models with which to compare our results. Previous studies in high-income country cities have identified traffic as the most important sources of NO_x emissions, just as we found in Accra [34, 50, 51]. While other combustion sources unique to SSA, such as household biomass use and trash burning, could represent non-negligible sources of NO_x emissions, our final models did not include household biomass fuel use as an important predictor. Similar to our results, other studies have also demonstrated a strong influence of climate and photochemistry (e.g. solar radiation, temperature and RH) on NO_x emissions [52]. Our model R^2s increased by 12% and 5% for NO_2 and NO, respectively, following the inclusion of meteorological and seasonal variables [40]. Compared to spatial-only models, our space-time models performed similar to some studies in China [36], Europe [34, 53], and South Africa, but better than others [37, 38, 54–56].

Based on the newly revised WHO annual air quality guideline, all residents of AMA were estimated to live in areas where NO_2 concentrations were far above the recommended health-based annual guideline. Even with the old guideline of 40 μg m^{-3}, still the exposure of almost the entire AMA's population (98%) did not meet the guideline (table S2). Other previous studies have also demonstrated a disproportionate share of poor air quality in low-income neighborhoods when compared to high-income areas [13, 57–60]. We found a similar trend in NO_2 exposure in Accra as well, with much lower concentrations in the more affluent neighborhoods. This is probably attributed to the higher traffic congestions and emissions in poorer communities and among those who live closer to main roads. Additionally, there could be a higher share of household and commercial biomass fuel use among low-income neighborhoods but our NO_2 model did not show significant contributions from this source. We acknowledge that the 2010 census biomass data might be outdated, but the overall trend in biomass usage in Ghana has been in decline [61]. Further, substantial disparities in greenspaces between sparsely populated affluent neighborhoods and densely populated poor communities could explain the relatively higher pollution in poorer neighborhoods. Yet, even with such significant disparity in exposure by SES, the median NO_2 levels in the wealthiest neighborhoods was more than six times higher than the current WHO annual guideline. This calls for a broader policy approach aimed at reducing air pollution emissions across board.

In Accra, concentrations of other pollutants like fine $PM_{2.5}$ and BC also remain detrimentally high [4, 62]. When our results are considered in the context of these other pollutants as well as the increasing urban population growth and economic expansion in the city [4, 62], the data call for an urgent need for equity-focused policy intervention to safeguard the health of Accra residents. These findings further highlight the need to address overall air quality in Accra using an integrated approach with emphasis on equity to reduce the existing within- and between-neighborhood exposure disparities. This will require systematic multisectoral framework that involves aspects related to road traffic emission reduction, environmental management, increasing urban green spaces, improvements to road infrastructure, support for green transportation and cleaner cooking fuels, and enforcement of existing air quality regulations. Our estimates for the non-Harmattan season provide clearer guide for key emission sources that need to be included in any air quality management or policy initiatives for reducing air pollution exposure in Accra and could serve as a roadmap for other cities in the West African region.

4.1. Strength and limitations

This is the first fine-scale space-time NO and NO_2 models developed for a major SSA city, a place where economic growth is making road traffic the dominant source of urban air pollution. We leveraged a large city-wide measurement campaign and provided weekly data over 50 m spatial resolution collected across a calendar year. The data laid the foundation for long-term mapping of inequalities in urban air pollution in a major and growing SSA city and could form the basis for climate and health impact assessments in the SSA context. Further, the data could help track policy interventions designed to improve air quality at the city-scale. Our approach and data sources can be readily replicated in other SSA cities where there is limited long-term city-wide data, especially on combustion related pollutants.

Our study has some limitations. We had no quantitative information on important traffic and other combustion related variables such as road surface material, traffic volume, diesel generator use, informal industries, community biomass use, and trash burning. Some of these data sources are unique to SSA and might improve the model performance if available and may have influenced the variable selection and model performance. Also, the timing of some predictor variables like land-use classification and census population did not align precisely with the timing of the measurement campaign, which may have affected model prediction. Nonetheless, our models performed as well as those conducted in other global studies.

5. Conclusion

In addition to $PM_{2.5}$ pollution, gaseous pollutants from combustion sources are rising in growing SSA cities and altering the air pollution mixture. We used large-scale measurement data to map NO and NO_2 concentrations at fine spatial and temporal resolution in the Accra metropolis. Model predictions show that NO and NO_2 concentrations are at unhealthy levels in city, with major contributions from road traffic. We also show that while the entire city is severely impacted, residents living in the inner core city, commercial areas, and those in poorer neighborhoods are at the greatest risk of exposure. These results, when combined with the emerging data on fine $PM_{2.5}$, BC, and noise pollution in Accra [4, 5, 48, 62–64] have provided comprehensive information for broader policy intervention and for evaluating the effectiveness of those actions to improve air quality in Accra and elsewhere in SSA.

Data availability statement

The data cannot be made publicly available upon publication because they are not available in a format that is sufficiently accessible or reusable by other researchers. The data that support the findings of this study are available upon reasonable request from the authors.

Acknowledgments

We thank the generous Accra residents who allowed us to install the monitors on their property, the staff at Physics Department at the University of Ghana for providing the field laboratory space, and the Ghana Meteorology Agency for the rainfall data. This research was funded by the Pathways to Equitable Healthy Cities Grant from the Wellcome Trust [209376/Z/17/Z]. RA is supported by Health Effects Institutes' Rosenblith New Investigator Award (No. CR-83590201). For the purpose of open Access, the author has applied CC BY public copyright license to any Author Accepted Manuscript version arising from this submission.

ORCID iDs

Sierra N Clark https://orcid.org/0000-0002-8592-3466
Allison F Hughes https://orcid.org/0000-0002-9912-6935
Ricky Nathvani https://orcid.org/0000-0002-4488-5862
Raphael E Arku https://orcid.org/0000-0001-8914-8463

References

[1] The State of Global Air 2022 *How Does Your Air Measure Up Against the WHO Air Quality Guidelines? A State of Global Air Special Analysis* (Health Effects Institute) (available at: https://www.stateofglobalair.org/sites/default/files/documents/2022-03/soga-special-analysis_0.pdf)

[2] Bailis R, Ezzati M and Kammen D M 2005 Mortality and greenhouse gas impacts of biomass and petroleum energy futures in Africa *Science* **308** 98–103

[3] Zhou Z *et al* 2014 Chemical characterization and source apportionment of household fine particulate matter in rural, Peri-urban, and urban West Africa *Environ. Sci. Technol.* **48** 1343–51

[4] Alli A S *et al* 2021 Spatial-temporal patterns of ambient fine particulate matter ($PM_{2.5}$) and black carbon (BC) pollution in Accra *Environ. Res. Lett.* **16** 074013

[5] Wang J *et al* 2021 Nitrogen oxides (NO and NO2) pollution in the Accra metropolis: spatiotemporal patterns and the role of meteorology *Sci. Total Environ.* **803** 149931

[6] Liousse C, Assamoi E, Criqui P, Granier C and Rosset R 2014 Explosive growth in African combustion emissions from 2005 to 2030 *Environ. Res. Lett.* **9** 035003

[7] Marais E A, Silvern R F, Vodonos A, Dupin E, Bockarie A S, Mickley L J and Schwartz J 2019 Air quality and health impact of future fossil fuel use for electricity generation and transport in Africa *Environ. Sci. Technol.* **53** 13524–34

[8] Marais E A and Wiedinmyer C 2016 Air quality impact of diffuse and inefficient combustion emissions in Africa (DICE-Africa) *Environ. Sci. Technol.* **50** 10739–45

[9] Dionisio K L, Arku R E, Hughes A F, Vallarino J, Carmichael H, Spengler J D, Agyei-Mensah S and Ezzati M 2010 Air pollution in Accra neighborhoods: spatial, socioeconomic, and temporal patterns *Environ. Sci. Technol.* **44** 2270–6

[10] Egondi T, Muindi K, Kyobutungi C, Gatari M and Rocklöv J 2016 Measuring exposure levels of inhalable airborne particles ($PM_{2.5}$) in two socially deprived areas of Nairobi *Kenya. Environ. Res.* **148** 500–6

[11] Knippertz P, Evans M J, Field P R, Fink A H, Liousse C and Marsham J H 2015 The possible role of local air pollution in climate change in West Africa *Nat. Clim. Change* **5** 815–22

[12] Marais E A, Jacob D J, Wecht K, Lerot C, Zhang L, Yu K, Kurosu T P, Chance K and Sauvage B 2014 Anthropogenic emissions in Nigeria and implications for atmospheric ozone pollution: a view from space *Atmos. Environ.* **99** 32–40

[13] Zhou Z, Dionisio K L, Arku R E, Quaye A, Hughes A F, Vallarino J, Spengler J D, Hill A, Agyei-Mensah S and Ezzati M 2011 Household and community poverty, biomass use, and air pollution in Accra, Ghana *Proc. Natl Acad. Sci.* **108** 11028–33

[14] Bahino J *et al* 2018 A pilot study of gaseous pollutants' measurement (NO_2, SO_2, NH_3, HNO_3 and O_3) in Abidjan, Côte d'Ivoire: contribution to an overview of gaseous pollution in African cities *Atmos. Chem. Phys.* **18** 5173–98

[15] Anenberg S C, Mohegh A, Goldberg D L, Kerr G H, Brauer M, Burkart K, Hystad P, Larkin A, Wozniak S and Lamsal L 2022 Long-term trends in urban NO_2 concentrations and associated paediatric asthma incidence: estimates from global datasets *Lancet Planet Health* **6** e49–e58

[16] World Health Organization 2021 WHO global air quality guidelines Particulate matter (PM 2.5 and PM 10), ozone, nitrogen dioxide, sulfur dioxide and carbon monoxide (available at: https://iris.who.int/bitstream/handle/10665/345329/9789240034228-eng.pdf?sequence=1) Licence:CC BY-NC-SA 3.0 IGO

[17] NASA 2021 *NASA Air Quality Observations from Space* (available at: https://airquality.gsfc.nasa.gov/no2/world/africa/accra)

[18] Haslett S L *et al* 2019 Remote biomass burning dominates southern West African air pollution during the monsoon *Atmos. Chem. Phys. Discuss.* **19** 1–23

[19] Heft-Neal S, Burney J, Bendavid E and Burke M 2018 Robust relationship between air quality and infant mortality in Africa *Nature* **559** 254–8

[20] Abera A, Malmqvist E, Mandakh Y, Flanagan E, Jerrett M, Gebrie G S, Bayih A G, Aseffa A, Isaxon C and Mattisson K 2021 Measurements of nox and development of land use regression models in an east-African city *Atmosphere* **12** 519

[21] Gebreab S Z, Vienneau D, Feigenwinter C, Bâ H, Cissé G and Tsai M Y 2015 Spatial air pollution modelling for a West-African town *Geospat. Health* **10** 205–14

[22] Ghana Statistical Service 2021 *Ghana 2021 Population and Housing Census General Report* (available at: https://census2021.statsghana.gov.gh/dissemination_details.php?disseminatereport=MjYzOTE0MjAuMzc2NQ==&Publications#)

[23] Nathvani R *et al* 2022 Characterisation of urban environment and activity across space and time using street images and deep learning in Accra *Sci. Rep.* **12** 1–16

[24] Sather M E, Slonecker E T, Mathew J, Daughtrey H and Williams D D 2007 Evaluation of ogawa passive sampling devices as an alternative measurement method for the nitrogen dioxide annual standard in El Paso, Texas *Environ. Monit. Assess.* **124** 211–21

[25] Sather M E, Terrence Slonecker E, Kronmiller K G, Williams D D, Daughtrey H and Mathew J 2006 Evaluation of short-term Ogawa passive, photolytic, and federal reference method sampling devices for nitrogen oxide s in El Paso and Houston, Texas *J. Environ. Monit.* **8** 558–63

[26] Moodley K G, Singh S and Govender S 2011 Passive monitoring of nitrogen dioxide in urban air: a case study of Durban metropolis, South Africa *J. Environ. Manage.* **92** 2145–50

[27] OpenStreetMap 2019 (available at: https://www.openstreetmap.org/relation/192781#map=11/5.6336/-0.2259)

[28] The World Bank 2014 Land Cover Classification of Accra, Ghana (available at: https://datacatalog.worldbank.org/search/dataset/0039825)

[29] The United States Geological Survey 2020 *Landsat Normalized Difference Vegetation Index* (available at: https://www.usgs.gov/landsat-missions/landsat-normalized-difference-vegetation-index)

[30] Price R and Hallas M 2019 Mapping every building and road in sub-Saharan Africa *AGU Fall Meeting Abstracts (1 December 2019)* p IN41A-02 (available at: https://ui.adsabs.harvard.edu/abs/2019AGUFMIN41A..02P/abstract)

[31] Ghana Statistical Service 2010 *Population and Housing Census* (available at: https://www.statsghana.gov.gh/gssmain/storage/img/marqueeupdater/Census2010_Summary_report_of_final_results.pdf)

[32] National Oceanic and Atmospheric Administration (NOAA) (available at: https://www.ready.noaa.gov/data/archives/gdas1/)

[33] Abernethy R C, Allen R W, McKendry I G and Brauer M 2013 A land use regression model for ultrafine particles in Vancouver, Canada *Environ. Sci. Technol.* **47** 5217–25

[34] Beelen R *et al* 2013 Development of NO_2 and NOx land use regression models for estimating air pollution exposure in 36 study areas in Europe—The ESCAPE project *Atmos. Environ.* **72** 10–23

[35] De Hoogh K *et al* 2013 Development of land use regression models for particle composition in twenty study areas in Europe *Environ. Sci. Technol.* **47** 5778–86

[36] Lee J H, Wu C F, Hoek G, de Hoogh K, Beelen R, Brunekreef B and Chan C-C 2014 Land use regression models for estimating individual NOx and NO_2 exposures in a metropolis with a high density of traffic roads and population *Sci. Total Environ.* **472** 1163–71

[37] Lee M et al 2017 Land use regression modelling of air pollution in high density high rise cities: a case study in Hong Kong Sci. Total Environ. 592 306–15
[38] Saucy A et al 2018 Land use regression modelling of outdoor NO_2 and $PM_{2.5}$ concentrations in three low income areas in the western cape province, South Africa Int. J. Environ. Res. Public Health 15 1452
[39] Bates D, Mächler M, Bolker B and Walker S 2015 Fitting linear mixed-effects models using lme4 J. Stat. Softw. 67 1–48
[40] Anand J S and Monks P S 2017 Estimating daily surface NO_2 concentrations from satellite data—A case study over Hong Kong using land use regression models Atmos. Chem. Phys. 17 8211–30
[41] Lee H J and Koutrakis P 2014 Daily Ambient NO_2 concentration predictions using satellite ozone monitoring instrument NO_2 data and land use regression Environ. Sci. Technol. 48 140204134232009
[42] van Nunen E et al 2017 Land use regression models for ultrafine particles in six European areas Environ. Sci. Technol. 51 3336–45
[43] Proietti E, Delgado-Eckert E, Vienneau D, Stern G, Tsai M Y, Latzin P, Frey U and Röösli M 2016 Air pollution modelling for birth cohorts: a time-space regression model Environ. Health 15 61
[44] Shi Y, Bilal M, Ho H C and Omar A 2020 Urbanization and regional air pollution across South Asian developing countries—A nationwide land use regression for ambient $PM_{2.5}$ assessment in Pakistan Environ. Pollut. 266 115145
[45] Wang M, Sampson P D, Hu J, Kleeman M, Keller J P, Olives C, Szpiro A A, Vedal S and Kaufman J D 2016 Combining land-use regression and chemical transport modeling in a spatiotemporal geostatistical model for ozone and $PM_{2.5}$ Environ. Sci. Technol. 50 5111–8
[46] Yang B-Y et al 2019 Ambient PM1 air pollution and cardiovascular disease prevalence: insights from the 33 communities Chinese health study Environ. Int. 123 310–7
[47] Zhang X, Just A C, Hsu H H L, Kloog I, Woody M, Mi Z, Rush J, Georgopoulos P, Wright R O and Stroustrup A 2021 A hybrid approach to predict daily NO_2 concentrations at city block scale Sci. Total Environ. 761 143279
[48] Clark S N et al 2022 Spatial modelling and inequalities of environmental noise in Accra, Ghana Environ. Res. 214 113932
[49] Gong C, Xian C, Wu T, Liu J and Ouyang Z 2023 Role of urban vegetation in air phytoremediation: differences between scientific research and environmental management perspectives npj Urban Sustain. 3 1–15
[50] Lu M, Soenario I, Helbich M, Schmitz O, Hoek G, van der Molen M and Karssenberg D 2020 Land use regression models revealing spatiotemporal co-variation in NO_2, NO, and O_3 in the Netherlands Atmos. Environ. 223 117238
[51] Rahman M M, Yeganeh B, Clifford S, Knibbs L D and Morawska L 2017 Development of a land use regression model for daily NO_2 and NOx concentrations in the Brisbane metropolitan area, Australia Environ. Modelling Softw. 95 168–79
[52] Seinfeld J H and Pandis S N 2016 Atmospheric Chemistry and Physics: From Air Pollution to Climate Change (Wiley)
[53] Eeftens M et al 2016 Development of land use regression models for nitrogen dioxide, ultrafine particles, lung deposited surface area, and four other markers of particulate matter pollution in the Swiss SAPALDIA regions Environ. Health 15 1–14
[54] Henderson S B, Beckerman B, Jerrett M and Brauer M 2007 Application of land use regression to estimate long-term concentrations of traffic-related nitrogen oxides and fine particulate matter Environ. Sci. Technol. 41 2422–8
[55] Liu C, Henderson B H, Wang D, Yang X and Peng Z R 2016 A land use regression application into assessing spatial variation of intra-urban fine particulate matter ($PM_{2.5}$) and nitrogen dioxide (NO_2) concentrations in City of Shanghai China Sci. Total Environ. 565 607–15
[56] Muttoo S, Ramsay L, Brunekreef B, Beelen R, Meliefste K and Naidoo R N 2018 Land use regression modelling estimating nitrogen oxides exposure in industrial south Durban, South Africa Sci. Total Environ. 610–611 1439–47
[57] Demetillo M A G et al 2020 Observing nitrogen dioxide air pollution inequality using high-spatial-resolution remote sensing measurements in Houston, Texas Environ. Sci. Technol. 54 9882–95
[58] Levy J, Dumyahn T and Spengler J 2002 Particulate matter and polycyclic aromatic hydrocarbon concentrations in indoor and outdoor microenvironments in Boston, Massachusetts J. Expos. Sci. Environ. Epidemiol. 12 104–14
[59] Perlin S A, Sexton K and Wong D W S 1999 An examination of race and poverty for populations living near industrial sources of air pollution J. Expos. Sci. Environ. Epidemiol. 9 29–48
[60] Perlin S A, Wong D and Sexton K 2001 Residential proximity to industrial sources of air pollution: interrelationships among race, poverty, and age J. Air Waste Manage. Assoc. 51 406–21
[61] Arku R E, Bennett J E, Castro M C, Agyeman-Duah K, Mintah S E, Ware J H, Nyarko P, Spengler J D, Agyei-Mensah S and Ezzati M 2016 Geographical inequalities and social and environmental risk factors for under-five mortality in Ghana in 2000 and 2010: Bayesian spatial analysis of census data PLoS Med. 13 1–14
[62] Alli A S et al 2023 High-resolution patterns and inequalities in ambient fine particle mass ($PM_{2.5}$) and black carbon (BC) in the Greater Accra Metropolis Ghana Sci. Total Environ. 875 162582
[63] Clark S N et al 2020 High-resolution spatiotemporal measurement of air and environmental noise pollution in sub-Saharan African cities: pathways to equitable health cities study protocol for Accra, Ghana BMJ Open 10 e035798
[64] Clark S N et al 2021 Space-time characterization of community noise and sound sources in Accra, Ghana Sci. Rep. 11 1–14